Galvanomagnetic Properties and Anomalous Hall Effect of n-InSb single Crystal and its Device

G. M. Mahmoud and F. S. Terra

Solid State Physics Department, Physical Research Division, National Research Centre, 33 El-Bohouth St., Dokki, Giza, 12622, Egypt.

Hall effect experimental procedures was used for determining the electrical resistivity, electron mobility (μ_e), carrier concentration (η), magnetoresistance (MR) and anomalous Hall effect (AH) as a function of temperature .The obtained curves are discussed in detail. The AH effect is defined as the zero field extrapolation of the high field data. An experiment illustrates the magnetic sensing ability of InSb single crystal was designed, where the InSb resistance value changed under applying external direct magnetic field, for insuring the high sensitivity to the magnetic field of such III-V material.

1. Introduction:

InSb is a crystalline compound composed of the elements indium and antimony. It has a dark grey silvery appearance for metal pieces or powder with vitreous luster, melts and decomposes if subjected to a temperature over 500°C, hence, liberates antimony and antimony oxide vapors [1]. The binary intermetallic compound InSb was synthesized earlier in 1929 with a zinc blende structure. Indium antimonide (InSb) is one of the III-V group with low energy band gap semiconductor, low effective mass (0.014 m_e), and high electron mobility (7–8 × 10^4 $cm^2V^{-1}s^{-1}$) at RT [2, 3]. So, InSb material is considered as the best suited for Hall purposes [4] and magnetoresistance (MR) devices. The sensitivity of a Hall element is inversely dependent on its thickness [5]. Generally, as the InSb film thickness increases, the threading dislocation density decreases and therefore the electron mobility increase [6].

In 1995, many Hall sensors were manufactured around the world. Due to the need for highly sensitive sensors, since forth, about 80% of Hall sensors, usually, are made of InSb [7]. Due to its low band gap , it has been particularly attraction as a potential material in case of high performance devices, low temperature diodes, infrared IR detectors, laser devices [8-10] or light emitting diodes (LEDs) if the doping material (Si, Mg) are controlled well [11], X-ray monochromatic detector, optical-immersion lenses as well as magnetic sensors. InSb has attracting great interest as a material for mid-IR applications, with cutoff wavelength about 7.3 μm at 300 K [12].

From other studies magnetized InSb is also promising as photonic crystal, metamaterial, and plasmonics [13]. Besides, amongst the optical Hall effect (OHE) materials[14], the III-V semiconductors are also promising where it has guaranteed smallest energy band gap E_g =0.18 eV at room temperature, the highest electron mobility μ_e =78,000 cm^2 /Vs, the smallest electron effective mass $m_e^* = 0.015m_e$. As a result, InSb has been expected to be a key role material for realizing terahertz devices [15], and radiation detectors [16].

In general, such Hall sensors with an active area of micron and submicron square are fabricated from various metals (Au, Al), alloys (NiFe), (FePt), semimetals (Bi), semiconductors (InSb), (InAs) on the basis of two-dimensional electron gas and graphene [17].

In the InSb crystals, the concentration of electrons differs according to the doping admixture material (S, Se, and Te). It has been established that, InSb single crystals of electron concentrations up to 1.5x 10^{19} **c**m^{-3} can be, easily, grown from the zone melting by doping with InTe [18]. As a result for such unique optical and electrical characteristics; highest number of intrinsic electron mobility and the narrowest band gap [19]; the indium antimonide is more suitable for the long-wavelength photodetectors and the diluted magnetic semiconductor [20]. InSb sensors exhibit high efficiency in militarical purposes such as the thermal imaging cameras and the aerospace applications. The great performance of InSb magnetic sensors expand till the speed and rotation angle detectors in the automotives [21], cellular phones, where III-V materials act as microwave transistors, also, in the compact disks [22]. Now, III-V compounds become remarkable ferromagnetic materials by doping them with magnetic elements i.e. Mn, Fe and Co. [23].

For the thin or thick (bulk in some cases) films, if a current "I" flows in a film plane then a perpendicular magnetic field H is applied to the film, a Hall voltage (VH) appears traversing to both I and H. Such voltage is due to Lorentz forces (F) acted on the charge carriers "e" moving by velocity "v". If the film material is magnetic, thus, an extraordinary contribution would appear taking proportional orientation to the component of the magnetization M along z−direction and perpendicular to the material plane, through the constant coefficient R_{AHE} :

$$V_H/I=R_0H+R_{AHE}M_z \quad (1)$$

where, R_0 represents the ordinary Hall coefficient and R_{AHE} anomalous (or extraordinary) Hall coefficients (AH) [24].

Weiss [25] has studied the galvanomagnetic properties of InSb semiconducting single crystal with high electron mobility. They reported that the coefficient is not dependent on the magnetic field specially at high values of magnetic field .He has investigated the variation of the electrical conductivity and the Hall coefficient in the temperature range from 90 to 470 K.

Tanenbaun et al. [26] have measured Hall effect and conductivity of InSb single crystals of both n- and p-types, from 100 – 500 K, their results are in accordance with ours. Jung et al. [27] have studied the conductivity, Hall coefficient and Hall mobility of InSb single crystals as a function of temperature from 90 – 470K, in accordance with us.

In our present work we aimed to study the electrical resistivity, the charge carriers concentration and the charge carriers mobility as a function of temperature from 100 – 450 K beside the anomalous Hall effect for our n- InSb single crystalline sample. The energy dispersive X-ray analysis, EDX was carried out to confirm our sample composition. Moreover we spotted on its high ability for sensing lowest change happening in the magnetic field, supporting our results with a photographed experiment bolstering this intensive magnetic sensing property.

2. Experimental Work:

In this work Quanta FEG 250 attached to the scanning electron microscope was used to check the compositional analysis (EDX) of InSb single crystal wafer.

The electrical resistivity was measured with high impedance electrometer (model, Keithly 617). An evacuated metallic cryostat (model CROYO industry, USA supplied with a heater and a platinum sensor) was used. An automatic temperature controller (model, Lake Shore, 321, USA) connected with the cryostat was used for measuring the galvanomagnetic properties as a function of temperature

The sample geometry is represented in Fig.(1), where the direction 1-2 represents the current path, the directions 3-5 and 4-6 are used to measure the resistance in two parallel directions along the current path direction .The Hall voltage is measured along the directions 3-4 and 5-6, which are perpendicular to both the current and the magnetic field directions, assuming that the current and the magnetic field are perpendicular to each other.

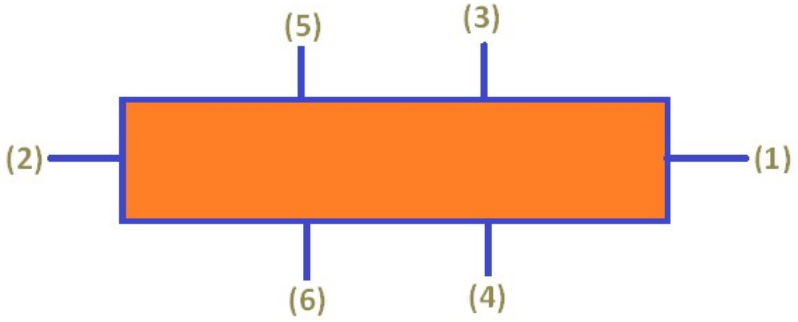

Fig. (1): Hall Sample geometry.

The circuit for InSb magnetic sensor experiment is composed of a d.c. power supply (Model: PE 1535 DC power supply), electromagnetic coil, a multimeter (Model: M890C^{+}) to measure the change in resistance , of our sensor, due to the application of the magnetic field. Finally, a Gauss meter (Model: Oxford Instruments 5200, Hall Effect Magnetometer) whose sensor is put just at the electromagnet was used.

3. Results and discussions:

3.1. Energy Dispersive X- ray analysis (EDX)

Figure (2) shows the EDX result of InSb single crystal. The atomic ratio of In: Sb is 43.75:56.25, indicating a slight deviation from the stoichiometric composition, with Sb excess.

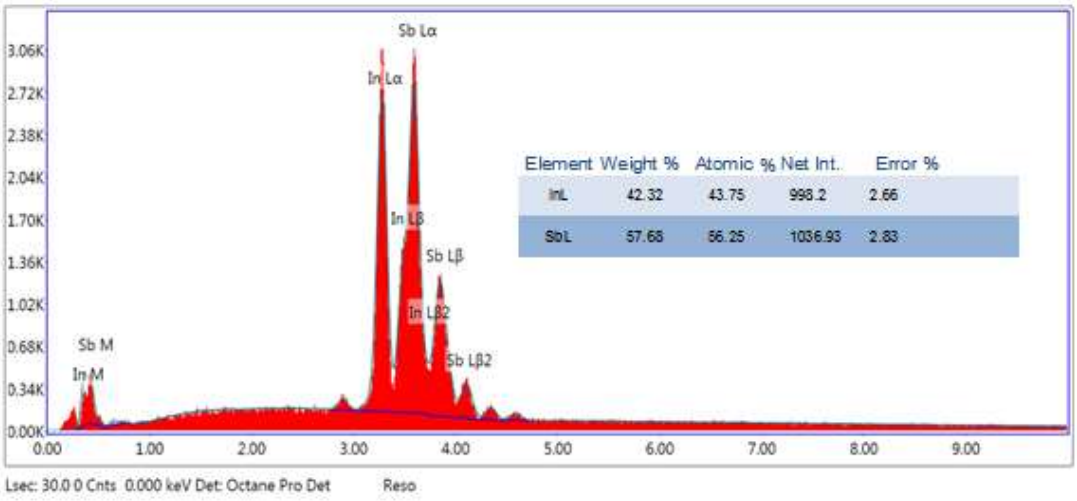

Fig. (2): The EDX result of InSb single crystal.

3.2. Galvanomagnetic and Anomalous Hall (AH) Resistivity Results

Figure (3) shows the dependence of the electrical resistivity, ρ on the reciprocal of the temperature ,1000/T(K^{-1}) along two parallel directions as shown in the sample geometry Fig.(1) in the current direction.

The electrical resistivity ρ_{35} was found to decrease from 0.251 Ω .cm at temperature 106.4 K to 0.0011 Ω .cm at 340K indicating a semicon- ducting nature, which agrees with Tanenbaun et al. [26] and Jung et al [27]. Both ρ_{35} and ρ_{46} possess the same behavior except that ρ_{35} is slightly higher than ρ_{46}.

Figure (4) shows the variation of the charge carriers concentration with temperature along two parallel directions 3-4 and 5-6 perpendicular to both the current and the magnetic field directions . It is interesting to observe that both curves coincide on each other, which informs us about the uniformity of charge

carriers distribution in n-InSb single crystal .It is noticed that the number of the carriers concentration (n) increases from $1.23X10^{14}$ at 106.4 K to $9.77X10^{16}$ at 400K.,i.e. by about three orders of magnitude. This means that the Hall coefficient, R_H decreases with heating as reported in references [25] and [27].

The charge carriers mobility, μ as a function of temperature is represented in Fig. (5). It is taken in consideration that , $\mu_{346} = R_{H\,34} / \rho_{46}$ and $\mu_{456} = R_{H\,56} / \rho_{46}$,where $R_{H\,34}$ is the Hall coefficient along 3-4 direction of the sample and $R_{H\,56}$ is that along 5-6 sample. The values of the carriers mobility decreases from $1.5X10^{6}$ at 106.4 K to $2X10^{4}$ at 400K, i.e. by about two orders of magnitude. The decrease of mobility with heating is reported in Ref. [26].

The anomalous Hall resistivity, ρ_{AH} as a function of temperature is presented in Fig.(6). We remember that the anomalous Hall voltage is defined as the zero magnetic field extrapolation of the high field data. It is observed that the anomalous Hall voltage decreases from 1.457 Ω.cm at 106K to 1.011 Ω.cm at 235K, then the increment in the values became slight till reaching 0.00231 Ω.cm at 400K.

The variation of the magnetoresistance, MR with temperature of our n-InSb sample is represented in Fig.(7), in which the value of MR decreases from 0.367 at 106.4 K to 0.00018 at 340K. It is observed that the behavior of the MR resembles that of ρ as a function of temperature. Therefore the MR works better at lower temperatures than that at higher temperatures.

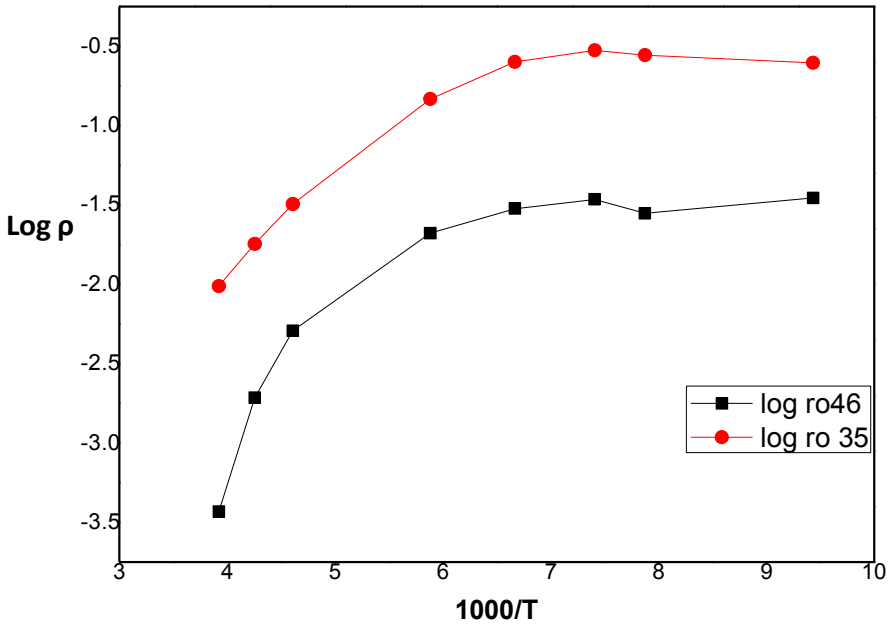

Fig. (3): The dependence of the electrical resistivity, ρ on the reciprocal of the temperature ,1000/T(K^{-1})

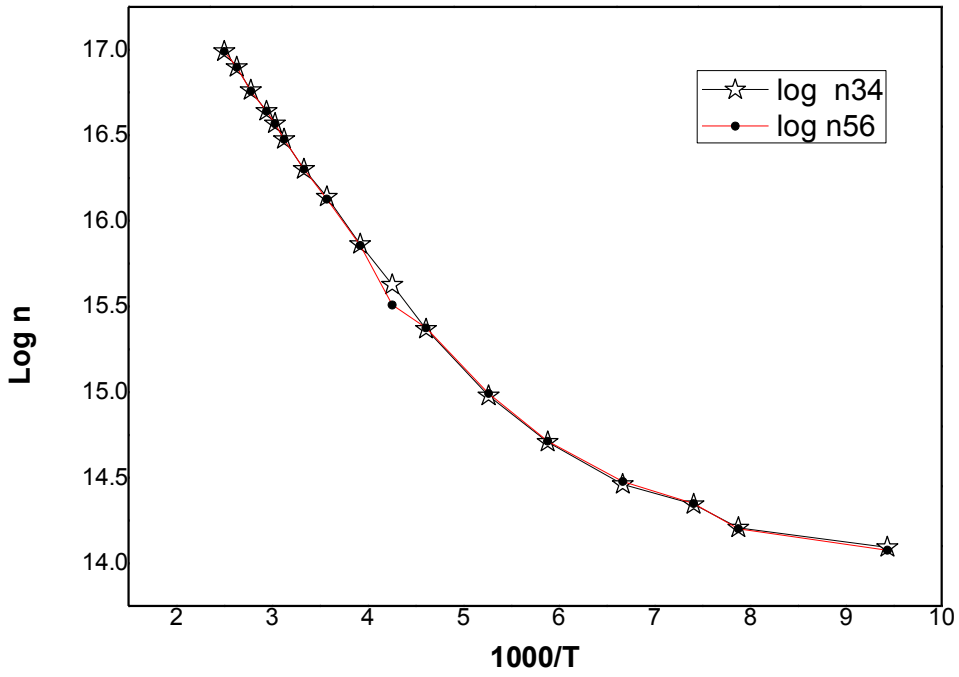

Fig.(4): The variation of charge carriers concentration with temperature

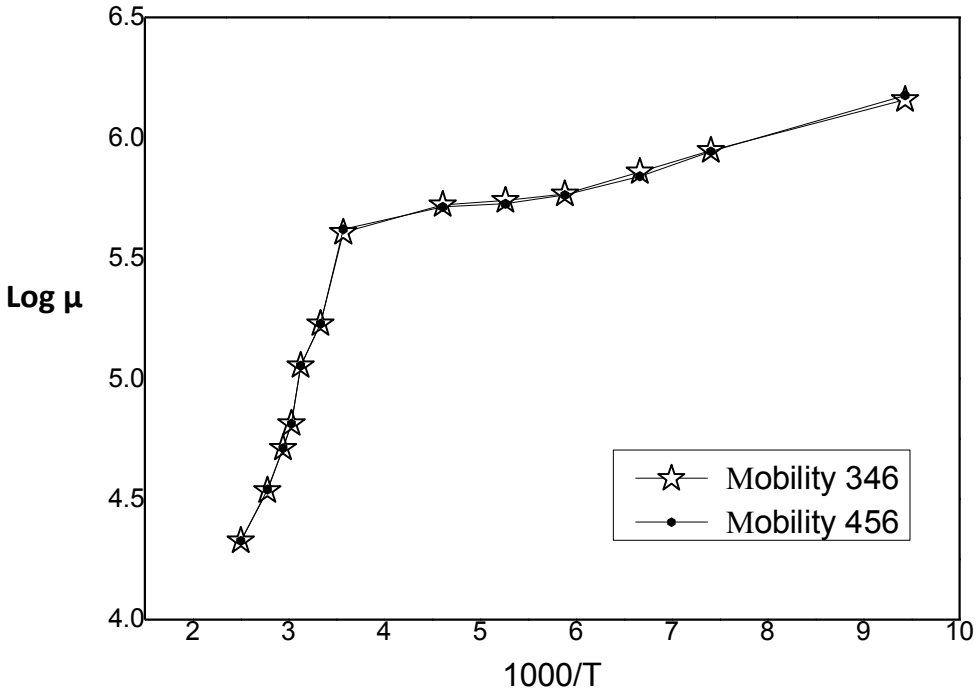

Fig. (5): The charge carriers mobility, μ as a function of temperature.

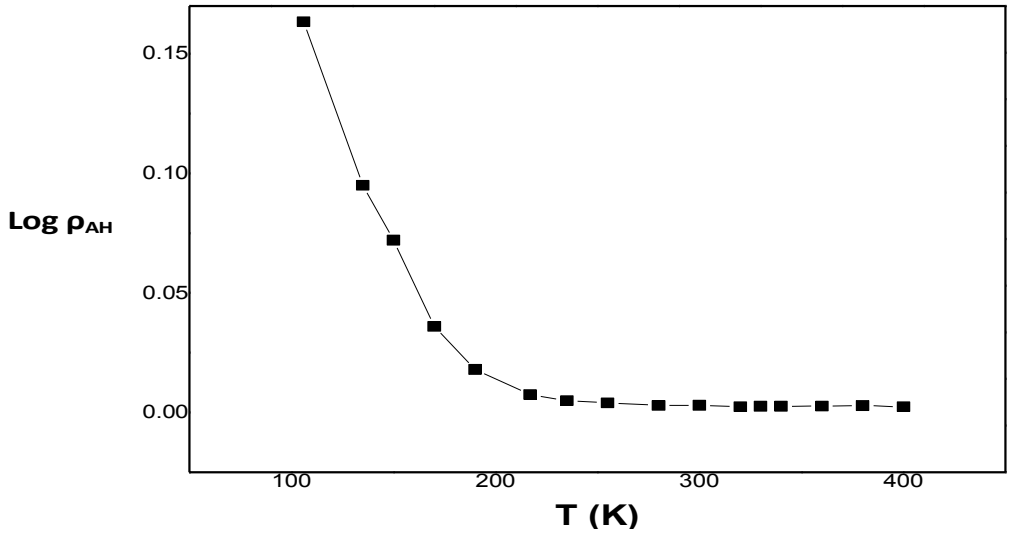

Fig.(6): The anomalous Hall resistivity, ρ_{AH} as a function of temperature.

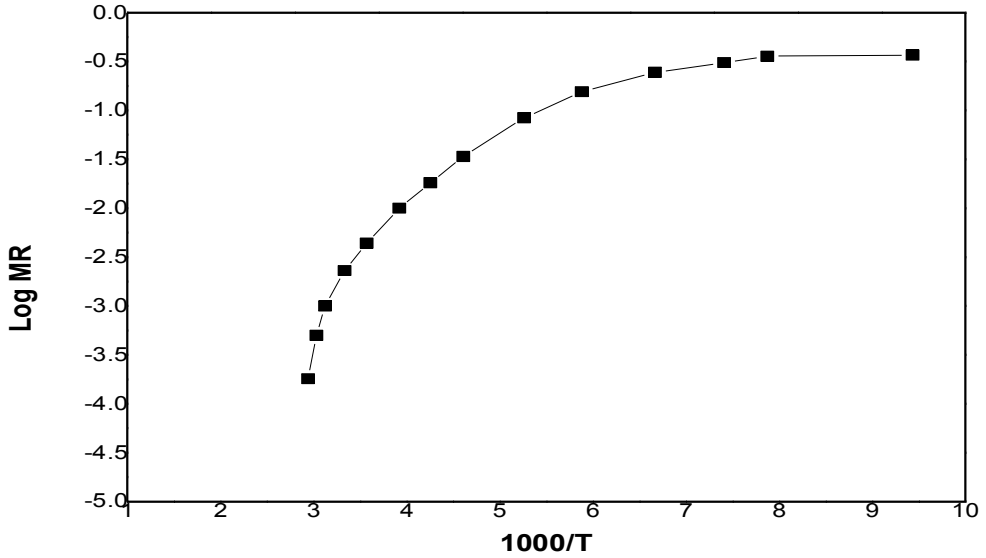

Fig.(7): variation of the magneto resistance, MR with temperature.

3.3. InSb Device :

In this section we explain how the InSb single- crystal device is sensitive to a slight variation of the magnetic field. Fig.(8) shows the photographic view taken for our InSb test sample, where a) denotes the device before applying the magnetic field , b) after applying the magnetic field and c) zoomed view, which illustrates the device in the electric circuit; orangey arrow points to the InSb device; indicated by No. 1)to the Gauss meter and its probe by No. 2), where, No. 3) shows the DC power supply with Maximum output DC voltage 40 V and 500 mA, and 4)to a dielectric fiber board, which carries, at its middle, the red coil with siliconic wrought iron core, put in front of one side the probe while our device for the other side.

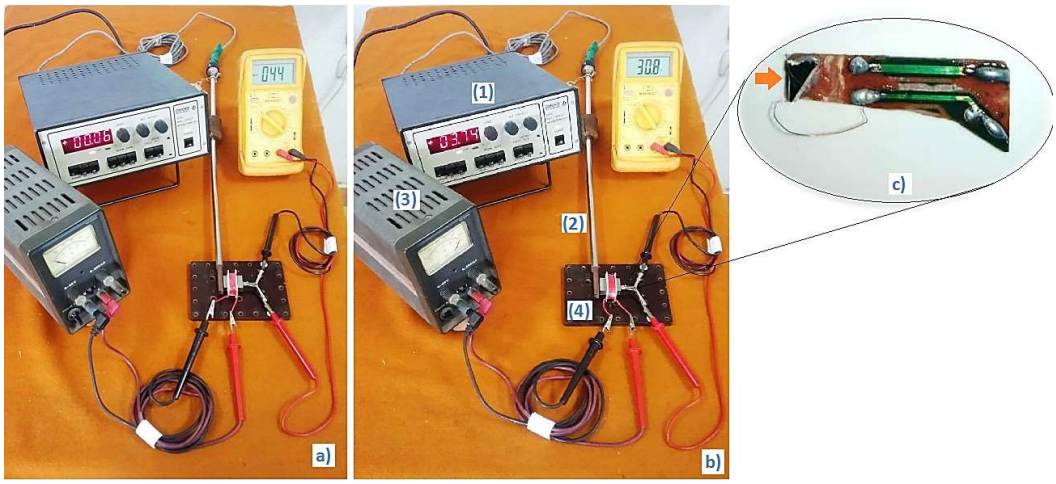

Fig.(8): InSb Device testing experiment.

At first, part a) in Fig. (8) before applying any field, the circuit is switched off, the Gauss meter shows the value 00.06 mT (6 Gauss), at zero voltage. The multi-meter shows the initial value of the resistance 44 Ω before applying external magnetic field. In part b) after applying the magnetic field created by a gradual increase of the current across the coil.

Figure (9) shows the results obtained by applying the current to the coil, leading to creation of a magnetic field and the resultant resistance of InSb test device.

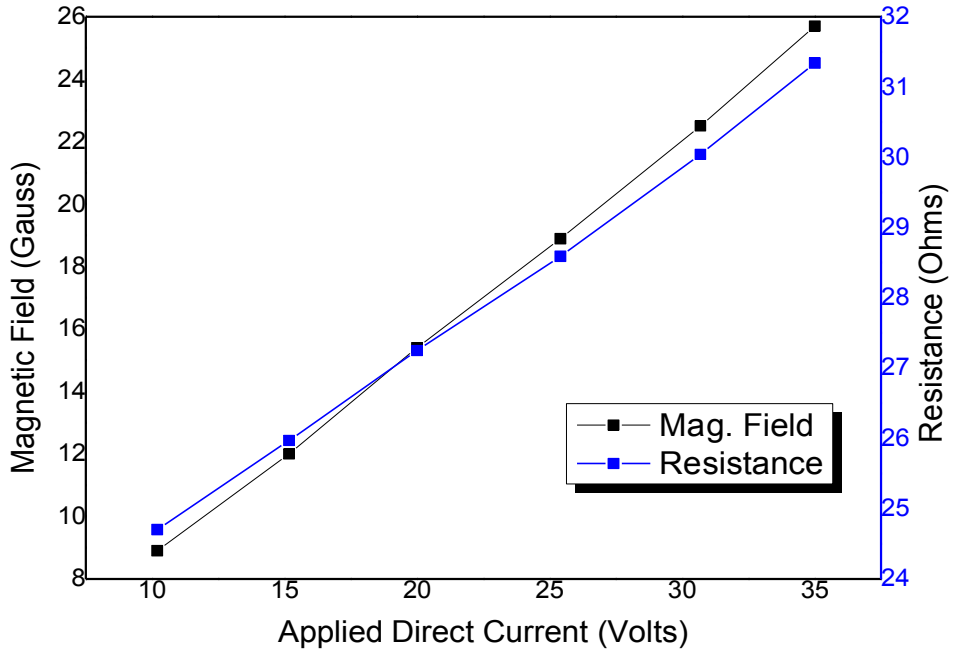

Fig. (9): Parameters of InSb device as a magnetic sensor.

4. Conclusions:

The galvanomagnetic properties and the anomalous Hall voltage of InSb single-crystal wafer were widely studied in the temperature range 100-450 K. **T**he galvanomagnetic properties include the electrical resistivity, the charge carriers concentration, the charge carriers mobility and the magnetoresistance. The electrical resistivity decreases with temperature increase indicating a semiconducting behavior. The resistivity decrease is due to the increase of the charge carriers concentration. The magnetoresistance decreases with temperature increase. Besides, the n-InSb single crystalline wafer can be used as a test magnetic sensing element even at low magnetic field.

Aknowledgement

The authors are grateful to Dr.Mahmoud Nasr ,Researcher in our Solid State Physics Department for helping us in making a test magnetic sensing element from InSb single crystal wafer .

References:

1. Farag, A. A. M., Terra, F. S., Fahim, G. M. M., & Mansour, A. M. (2012). Current transport and capacitance-voltage characteristics of n-InSb/p-GaP prepared by flash evaporation and liquid phase epitaxy. Metals and Materials International, 18(3), 509–515. doi:10.1007/s12540-012-3020-4

2. B. D. Gadkari and B. M. Arora, "*Characterization* of *p*and *n-type bulk InSb crystals grown* by *vertical directional solidification technique", INDIAN* J *PURE* & APPL PI-IYS, VOL 38, APRIL 2000, pp 237-242

3. Agrawal N. III-V group (InSb) dilute magnetic semiconductor. J Mod Appl Phys. Dec 2018;2(2):23-24

4. Lekwongderm, P., Chumkaew, R., Thainoi, S., Kiravittaya, S., Tandaechanurat, A., Nuntawong, N., … Panyakeow, S. (2019). Study on Raman Spectroscopy of InSb Nano-Stripes Grown on GaSb Substrate by Molecular Beam Epitaxy and Their Raman Peak Shift with Magnetic Field. Journal of Crystal Growth.doi:10.1016/j.jcrysgro.2019.02.033

5. Ohshita, M. (1994). InSb films for magnetic sensors. Sensors and Actuators A: Physical, 40(2), 131–134.doi:10.1016/0924-4247 (94)85018

6. Zhao, X., Zhang, Y., Guan, M., Cui, L., Wang, B., Zhu, Z., & Zeng, Y. (2017). Effect of InSb/In 0.9 Al 0.1 Sb superlattice buffer layer on the structural and electronic properties of InSb films. Journal of Crystal Growth, 470, 1–7.doi:10.1016/j.jcrysgro.2017.03.051

7. Kuze, N., & Shibasaki, I. (1997). MBE research and production of Hall sensors. III-Vs Review, 10(1), 28–32.doi:10.1016/s0961-1290(99)80054-4

8. Farag, A. A. M., Ashery, A., & Terra, F. S. (2008). Fabrication and electrical characterization of n-InSb on porous Si heterojunctions prepared by liquid phase epitaxy. Microelectronics Journal, 39(2), 253–260.doi:10.1016/j.mejo.2007.10.029

9. Farag, A. A. M., Terra, F. S., Mahmoud, G. M., & Mansour, A. M. (2009). Study of Gaussian distribution of inhomogeneous barrier height for n-InSb/p-GaAs heterojunction prepared by flash evaporation. Journal of Alloys and Compounds, 481(1-2), 427–433.doi:10.1016/j.jallcom.2009.03.004

10. Farag, A. A. M., Terra, F. S., Ashery, A., & Mansour, A. M. (2014). Structural and electrical characteristics of n-InSb/p-GaAs heterojunction prepared by liquid phase epitaxy. Journal of Alloys and Compounds, 615, 604–609.doi:10.1016/j.jallcom.2014.06.058

11. Götz, W., Kern, R. ., Chen, C. ., Liu, H., Steigerwald, D. ., & Fletcher, R. . (1999). Hall-effect characterization of III–V nitride semiconductors for high efficiency light emitting diodes. Materials Science and Engineering: B, 59(1-3), 211–217.doi:10.1016/s0921-5107(98)00393-6

12. Jia, B. W., Tan, K. H., Loke, W. K., Wicaksono, S., & Yoon, S. F. (2018). Growth and characterization of InSb on (1 0 0) Si for mid-infrared application. Applied Surface Science, 440, 939–945.doi:10.1016/j.apsusc.2018.01.219

13. Fan, F., Xu, S.-T., Wang, X.-H., & Chang, S.-J. (2016). Terahertz polarization converter and one-way transmission based on double-layer magneto-plasmonics of magnetized InSb. Optics Express, 24(23), 26431. doi:10.1364/oe.24.026431

14. Kühne, P., Herzinger, C. M., Schubert, M., Woollam, J. A., & Hofmann, T. (2014). Invited Article: An integrated mid-infrared, far-infrared, and terahertz optical Hall effect instrument. Review of Scientific Instruments, 85(7), 071301. doi:10.1063/1.4889920

15. Chochol, J., Postava, K., Čada, M., Vanwolleghem, M., Halagačka, L., Lampin, J.-F., & Pištora, J. (2016). Magneto-optical properties of InSb for terahertz applications. AIP Advances, 6(11), 115021.doi:10.1063/1.4968178

16. G. D. Bogomolov, V. V. Zav'yalov, E. A. Zotova, and E. Yu. Shamparov, A Fast Tunable Detector of Submillimeter Waves on Cyclotron Resonance in an InSb Crystal, Instruments and Experimental Techniques, Vol. 45, No. 1, 2002, pp. 78–86. Translated from Pribory i Tekhnika Eksperimenta, No. 1, 2002, pp. 87–95. Original Russian Text Copyright © 2002 by Bogomolov, Zav'yalov, Zotova, Shamparov.

17. Matveev, V. N., Levashov, V. I., Kononenko, O. V., Matveev, D. V., Kasumov, Y. A., Khodos, I. I., & Volkov, V. T. (2015). Hall effect sensors on the basis of carbon material. Materials Letters, 158, 384–387.doi:10.1016/j.matlet.2015.06.055

18. M.YA. DASHEVSKII, A. S. FILIPCHENKO and L. S. OKUN, Electrical Properties of Heavily Doped n-Type Indium Antimonid, phys. stat. sol. (a) 5, 597 (1971), Subject classification: 14.3; 13.4; 22.2.3, Academy of Sciences of the UflsR, Leningrad (b), Steel and Alloys Institute, Moscow (a), and A. F. Ioffe Physico-Technical Institute

19. Bolshakova, I., F.S. Terra, G.M. Mahmoud and A.M. Mansour, 2016. High quality InSb microcrystal hall sensor doped with Te or Bi. Int. J. Adv. Applied Phys. Res., 3: 5-10. DOI: 10.15379/2408-977X.2016.03.01.02

20. Koshihara, S., Oiwa, A., Hirasawa, M., Katsumoto, S., Iye, Y., Urano, C., … Munekata, H. (1997). Ferromagnetic Order Induced by Photogenerated Carriers in Magnetic III-V Semiconductor Heterostructures of (In,Mn)As/GaSb. Physical Review Letters, 78(24), 4617–4620.doi:10.1103/physrevlett.78.4617

21. Peng, W. L., Zhang, J. Y., Luo, L. S., Feng, G. N., & Yu, G. H. (2019). The ultrasensitive anomalous Hall effect induced by interfacial oxygen atoms redistribution. Journal of Applied Physics, 125(9), 093906.doi:10.1063/1.5084318

22. Ohno, H. (1998). Making Nonmagnetic Semiconductors Ferromagnetic. Science, 281(5379), 951–956.doi:10.1126/science.281.5379.951

23. T. Jungwirth, Qian Niu , and A. H. MacDonald, Anomalous Hall effect in ferromagnetic semiconductors, Physical review letters, 2002

24. Fasasi, T. A., Ruotolo, A., Zhao, X. W., Leung, C. W., & Lin, K. W. (2019). Photo-induced anomalous Hall effect in nickel thin films. Journal of Magnetism and Magnetic Materials, 485, 82–84. doi:10.1016/j.jmmm.2019.04.075

25. Weiss H.,J .Applied Phys., 32,10(1961)2064.doi/abs/10.1063/1.1777018.

26. Tanenbaun, M and Matta J.P. Letters To The Editor (1955) 1009- 1010.

27. Jung, Y. J., Park ,M. K., Tae S. I., Lee K. H., and Lee, H.J., J. Appl. Phys.,Vol.69,No.5(1991)3109-3114.